# Wideband Wearable Antenna

Pedro Guilherme Moreira Falcão
pedro.falcao@ist.utl.pt

Instituto Superior Técnico, Lisboa, Portugal

September 2021

***Abstract*—Antennas have a fundamental role in the functioning and evolution of society, as they are essential components of systems that enable the wireless transmission of information, over short and long distances. The theme of the dissertation was suggested by the Center for Nanotechnology and Technical, Functional and Intelligent Materials, CeNTI, within the scope of the iP Vest project [1]. This project consists in the development of intelligent protective clothing with two specific functions: the first to protect the user from aggressive weather conditions and the second will act in an active way containing all the sensing and communication for the protection and alert of the user. The proposed antenna system is intended to be integrated into this garment, making it possible to estimate the intensity of the incident electromagnetic field. This dissertation describes the analysis, design (with optimization), fabrication and testing of a set of printed monopoles, designed to work in the 700 MHz to 3.5 GHz band, with an input impedance of 50 Ω, with a reflection coefficient less than -10 dB for the entire working band and dual orthogonal linear polarization. The design procedure consisted of several simulations in the CST software of different configurations of the printed monopole in order to increase its bandwidth. The developed antennas have an absorber foam to mitigate the effects of the conductive shield that protects the user's body. The experimental results that it was possible to obtain (input reflection coefficient) show a good agreement with the numerical simulation results (CST), validating the design procedure followed and proving the concept of the proposed antenna.**

***Index Terms*—Antenna Monopole, Printed Antennas, Broadband Antenna, Wearable Antennas, System of Antennas, CeNTI, iP Vest**

## I. Introduction

Nowadays, wireless communications are an essential part of civilization. Sharing data is now faster, cheaper and more efficient. The traffic of information is growing fast over the years as the population and the number of internet users grow. With this growth, there is a need of improved coverage and better signal quality, resulting in more base stations and more electromagnetic radiation exposure. There is a considerable concern about the possible consequences to a human being exposed to electromagnetic fields over a long period. These high intensity fields are present in professional scenarios such as base stations since the intensity of electromagnetic fields is stronger in the emission and decays with distance. In that specific scenario, it is important to know the amplitude of the electromagnetic wave incident on the workers who maintain or install new antennas. The estimation of the intensity of such electromagnetic waves is the main objective of this thesis.

With the development of integrated circuit and printed circuit board (PCB) technology, printed antennas have drawn a lot of attention in the antenna R&D community. They are lightweight, low cost, robust, easy to fabricate and install. These antennas have a planar low profile and are versatile in terms of resonance frequency, radiation pattern, polarization and impedance. With so many advantages, printed antennas are a good candidate to be used in the proposed problem.

This thesis specific main goal is to design, fabricate and test a system of wearable wideband antennas with the purpose of measuring the amplitude of the electric field received by the user in a professional unknown work environment. The direction of the incident electric field into the user is undefined just like its polarization, therefore the system will work with space sectorization and probing of orthogonal polarizations. For each antenna it is requested dual linear polarization, an input impedance of 50 Ω and a reflection coefficient below -10 dB for the working bandwidth from 0,7 GHz to 3,5 GHz. The gain of the antenna is not a critical requirement since it is small or moderate, that is, as far as it reflects an adequate coverage of all sectors.

## II. State of the Art

The concept of microstrip antenna can be traced to 1953 by Deschamps and Sichak, when the authors developed a high resolution X-band antenna with a shaped vertical pattern and horizontal beam width of less than one degree. The microstrip patch we recognize today did not become well known until the 1970's through the work of Byron, Munson, and Howell. However, the work provided by Deschamps and Sichak presented new ways to think about the antenna structures and subsequent performance benefits and reductions in size, weight, and cost that could be realized through the use of microstrip or stripline transmission lines. In the four decades since, there are literally thousands of papers on this topic.

A microstrip antenna, which is a specific form of printed antenna, is a low-profile antenna that has many advantages: it is lightweight, inexpensive to fabricate, easy to feed, and easily

integrated with electronics. Radiation patterns are somewhat hemispherical, with a moderate directivity. It is usually flat and that´s why microstrip antennas are referred as planar antennas.

When a particular patch shape and mode are selected, they are very versatile in terms of resonance frequency, polarization, pattern, and impedance. Major disadvantages of microstrip antennas are their narrow bandwidth, low power, poor polarization purity, poor scan performance, spurious feed radiation and low efficiency. There are methods to increase the bandwidth and the efficiency, such as increasing the height of the substrate. However, as the height increases, surface waves are introduced which are not desirable as they extract power from the total available for direct radiation. Surface waves can be eliminated, while maintaining large bandwidths, by using cavities. Stacking is another method used to increase the bandwidth of microstrip elements. The bandwidth is inversely proportional to $\varepsilon_r$, meaning a foam substrate can provide a larger bandwidth [2, 3].

### *A. Printed Antennas*

In its most basic form, a microstrip antenna is manufactured with a flat plate over a ground plane. This antenna is built of printed circuit board material and the substrate makes up the patch antenna's dielectric. There are numerous dielectric substrates that can be used for the design of microstrip antennas, the ones that are most desirable for good antenna performance are thick substrates whose dielectric constant is in the lower end of the range because they provide better efficiency and larger bandwidth. Thin substrates with higher dielectric constants are desirable for microwave circuitry because they require tightly bound fields to minimize undesired radiation and coupling, and lead to smaller element sizes. Thicker substrate increases the gain to some extent, but may lead to undesired radiation pattern and coupling. A quite big challenge remains regarding this matter, if on one side antenna performance is important, on the other, circuit design is almost crucial, since printed antennas are regularly combined with other microwave circuits. The microstrip patch is designed so its pattern maximum is normal to the patch, this is accomplished by properly choosing the mode of excitation beneath the patch.

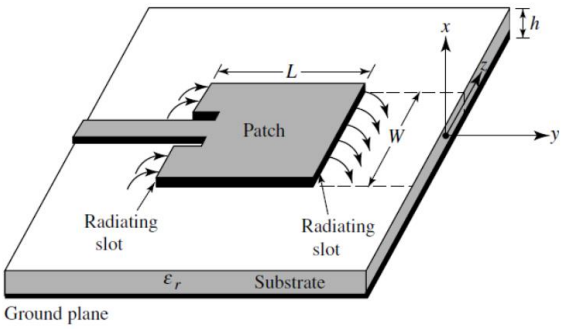


*Figure 1 - Microstrip antenna [2]*

Common microstrip antenna shapes are square, rectangular, thin strip (dipole), circular, elliptical, triangular, disc sector, circular ring and ring sector but any continuous shape is possible. The size of the ground plane is also important, a ground plane that is too small will result in a reduced front to back ratio. Making the ground plane larger increases the gain, but as the ground plane size increases, diffraction near the edges of the patch plays less of a role and increasing the size of an already "large" ground plane has very little effect on gain. Linear and circular polarizations can be achieved with either single elements or arrays of microstrip elements.

There are different configurations available that can be used to feed microstrip antennas, these methods can be contacting and non-contacting. In the contacting method the RF power is fed directly to the radiating patch using a connecting element such as a microstrip line. In the non-contacting method, power is transferred between the microstrip line and the radiating patch through electromagnetic coupling. The most popular feeding techniques are the microstrip line and the coaxial probe for contacting schemes, aperture coupling and proximity coupling for non-contacting schemes.

There are many methods of analysis for microstrip antennas. The most popular are the transmission line, cavity, and full wave among others. The transmission-line is the easiest solution and gives good physical insight, but is less accurate and it is more difficult to model coupling. The cavity model compared to the transmission-line model, is more accurate but at the same time more complex. It also gives good physical insight and is rather difficult to model coupling. The full wave models are very accurate and can treat single elements, finite and infite arrays, stacked elements, arbitrary shaped elements, and coupling but they are the most complex models and give less if any physical insight.

The transmission model will be used below. For the following study, a rectangular patch will be used, since is the most common configuration. A rectangular microstrip antenna can be represented as an array of two slots, each of width W and height h, separated by a distance L where L and W are the rectangular patch dimensions and h is the substrate thickness. Basically the transmission-line model represents the microstrip antenna by two slots, separated by a low-impedance $Z_c$ transmission line of length L as shown in figure 1.

#### *1) Analysis*

The transmission model will be used below. For the following study, a rectangular patch will be used, since is the most common configuration. Fringing fields have an important effect on the performance of a microstrip antenna. Due to the fact that the dimensions of the patch are finite along the length and width, the fields at the edges of the patch undergo fringing (principal mode). In microstrip antennas, the electric field in the center of the patch is zero, the radiation is due to the fringing field between the proximity of the patch and the ground plane. This is illustrated along the length in figure 2. The amount of the fringing field is a function of the dimensions of the patch and the height of the substrate. The higher the substrate, the larger the fringing field is.

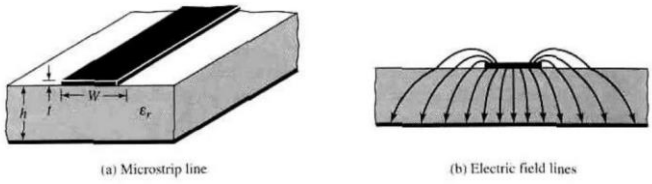


*Figure 2 - Microstrip antenna - Fringing effect [2]*

Since some waves travel in the substrate and some in air, an effective dielectric constant $\epsilon_{reff}$ is introduced to account for fringing and the wave propagation in the line. For low frequencies, the effective dielectric constant is constant. At intermediate frequencies, its values begin to increase and approach the values of the dielectric constant of the substrate. The expression for the effective dielectric constant can be defined as [2]:
For $W/h$>1

$$\epsilon_{reff} = \frac{\epsilon_r+1}{2} + \frac{\epsilon_r-1}{2}\left[1+12\frac{h}{W}\right]^{-\frac{1}{2}} \quad (1)$$

*2)* Effective Length, Resonant Frequency and Effective Width

The fringing effects make the patch looks larger than its physical dimensions. With that said, there are new dimensions when working with this type of antennas, called the effective length and effective width.

In figure 3 it is clear that the dimensions of the patch along its length have been extended on each end by a distance $\Delta L$, which is a functions of the effective dielectric constant $\epsilon_{reff}$ and the width-to-height ratio (W/h).

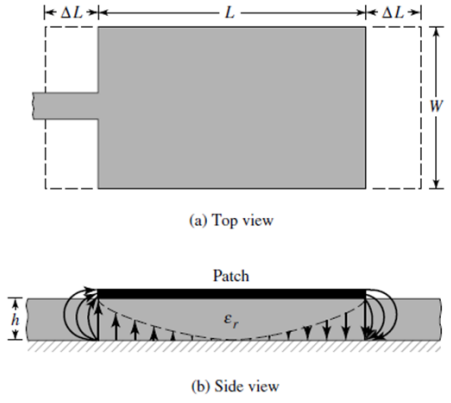


*Figure 3 - Microstrip patch - effective length due to fringing [2]*

A practical approximate relation for the horizontal extension of the length is [2]:

$$\frac{\Delta L}{h} = 0.412 \times \frac{(\epsilon_{reff}+0.3)\left(\frac{W}{h}+0.264\right)}{(\epsilon_{reff}+0.258)\left(\frac{W}{h}+0.8\right)} \quad (2)$$

Since the length of the patch has been extended by $\Delta L$ on each side, the effective length of the patch in now.

$$L_{eff} = L + 2\Delta L \quad (3)$$

For the dominant mode $TM_{010}$, the resonant frequency of the microstrip antenna is a function of its length. As $L = \lambda/2$ , it is given by:

$$f_{r_{010}} = \frac{1}{2L\sqrt{\epsilon_r}\sqrt{\mu_0\epsilon_0}} = \frac{c_0}{2L\sqrt{\epsilon_r}} \quad (4)$$

Where $c_0$ is the speed of light in free space. Since this resonance frequency does not account for fringing, it must be modified to include edge effects and should be computed using

$$f_{rc_{010}} = \frac{1}{2L_{reff}\sqrt{\epsilon_{reff}}\sqrt{\mu_0\epsilon_0}} = \frac{1}{2(L+2\Delta L)\sqrt{\epsilon_{reff}}\sqrt{\mu_0\epsilon_0}} \quad (5)$$

$$f_{rc_{010}} = q\frac{1}{2L\sqrt{\epsilon_r}\sqrt{\mu_0\epsilon_0}} = q\frac{c_0}{2L\sqrt{\epsilon_r}} \quad (6)$$

Where

$$q = \frac{f_{rc_{010}}}{f_{r_{010}}} \quad (7)$$

The q factor is referred to as the fringing factor. If we increase the substrate height h, the fringe effect also increases and leads to larger separations between the radiating edges, however by increasing the actual length of the patch, the resonance frequency decreases.

*3) Design*

A design procedure is outlined in [11] which leads to practical designs of rectangular microstrip antennas based on the formulation that has been described. The procedure assumes that the dielectric constant of the substrate ($\epsilon_r$), the resonant frequency ($f_r$), and the height of the substrate h values are known. The procedure is as follows:

1. Specify $\epsilon_r$, $f_r$ and h
2. For an efficient radiator, a practical width that leads to good radiation efficiencies is:
3. $$W = \frac{1}{2f_r\sqrt{\mu_0\epsilon_0}}\sqrt{\frac{2}{\epsilon_r+1}} = \frac{c_0}{2f_r}\sqrt{\frac{2}{\epsilon_r+1}} \quad (8)$$
   Where $c_0$ is the free space velocity of light.
4. Determine the effective dielectric constant of the microstrip antenna using equation (1)
5. Determine the length ΔL using equation (2)
6. The actual length of the patch can now be determined using equation (5).

*B. Printed Monopole Antenna*

In order to avoid some of the drawbacks of microstrip antennas, printed monopoles are introduced. The printed monopole antenna is included in a broad class of microstrip antennas. They have similar configuration but printed monopole antennas have a truncated ground plane providing larger bandwidth and nearly omnidirectional radiation characteristics. For proper matching of the printed monopole with the microstrip feed line, the dielectric constant and thickness of the substrate and the width of the feed need to be chosen carefully. Figure 4 represents the simplest configuration of the printed monopole, a thin microstrip, of width W, placed on top of the dielectric substrate, of height h, with the truncated ground plane on the other side.

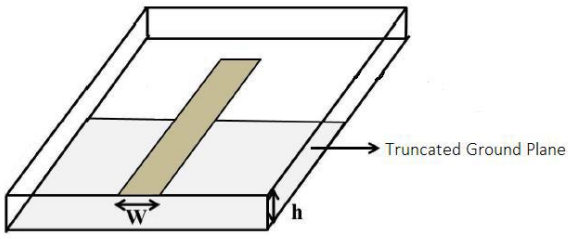


*Figure 4 - Simplest configuration of printed monopole*

Similar to microstrip patch antennas, the printed monopole can take many shapes regarding the patch geometry, for example, rectangular, triangular, circular, elliptical, octagonal, and others. Different geometries of the patch or the ground plane result mostly in variations in the return loss but to a lesser extent also of the gain and radiation pattern among the frequency band. [4]

### C. *Wearable Antennas*

In recent years, wearable antennas, have gained much attention due to all the practical applications and possibilities in enabling lightweight, flexible, low cost and portable wireless communication and sensing. A wearable antenna is meant to be a part of the clothing used for communication purposes, which includes tracking and navigation, mobile computing and public safety. The practical use of these antennas present some challenges, since they need to be capable of operating with minimum degradation in close proximity to the human body and need to be implemented using flexible materials and designed in a low profile structure. Size constraints, effects of structural deformation, fabrication complexity and accuracy are aspects that need to be considered when designing a wearable antenna. Despite slight variations in importance according to applications, most of these issues exist in the context of body-worn implementation.

Wearable antennas need to be designed to operate properly in the vicinity of human body. In addition, special attention must be paid to the Specific Absorption Rate (SAR), which aids in the quantitative study of power absorption issues required to meet the standards in order to avoid harming the human body. SAR quantifies the amount of EM radiation a human body can withstand without any health problems and is defined as the ratio between the transferred power and the mass (kg/lb) of the body where the values are being evaluated. [5, 6]

## III. Antenna Design and Optimization

The development of an antenna is a difficult process and can be resumed in five steps: design, simulation, optimization, fabrication and test. With the help of a software tool like CST (Computer Simulation Technology) Studio the design and optimization procedure is done through several simulations adjusting parameters values and components dimensions that influence the performance of the antenna.

The chosen material for the dielectric substrate was FR4, this being relatively cheap and easy to access despite introducing some losses. Since the antenna has to operate mainly at low frequencies this substrate is a good option because it performs poorly with increasing frequency. The FR4 substrate has a dielectric constant $\varepsilon_r = 4,3$ and loss tangent tan $\delta = 0,025$. For all simulations, a thickness of h=1,6 mm was chosen for the substrate.

### A. *Optimization Procedure for the Free Space Monopole*

Different configurations were simulated for the printed monopole, starting with the simplest of all, a straight strip. After obtaining some information about the line width, a microstrip patch antenna was also simulated. Looking for larger bandwidth and better performance new patch configurations were tested, namely a square patch, a trapezoidal patch, an inverted trapezoidal patch and finally an octagonal patch. For some configurations, changes to the ground plane and patch were simulated. Regarding the ground plane, these changes consisted of coplanar configurations or changes in the geometry of the conventional ground plane. For the patch, the changes consisted on inserting slots or adding triangular plates (figure 5).

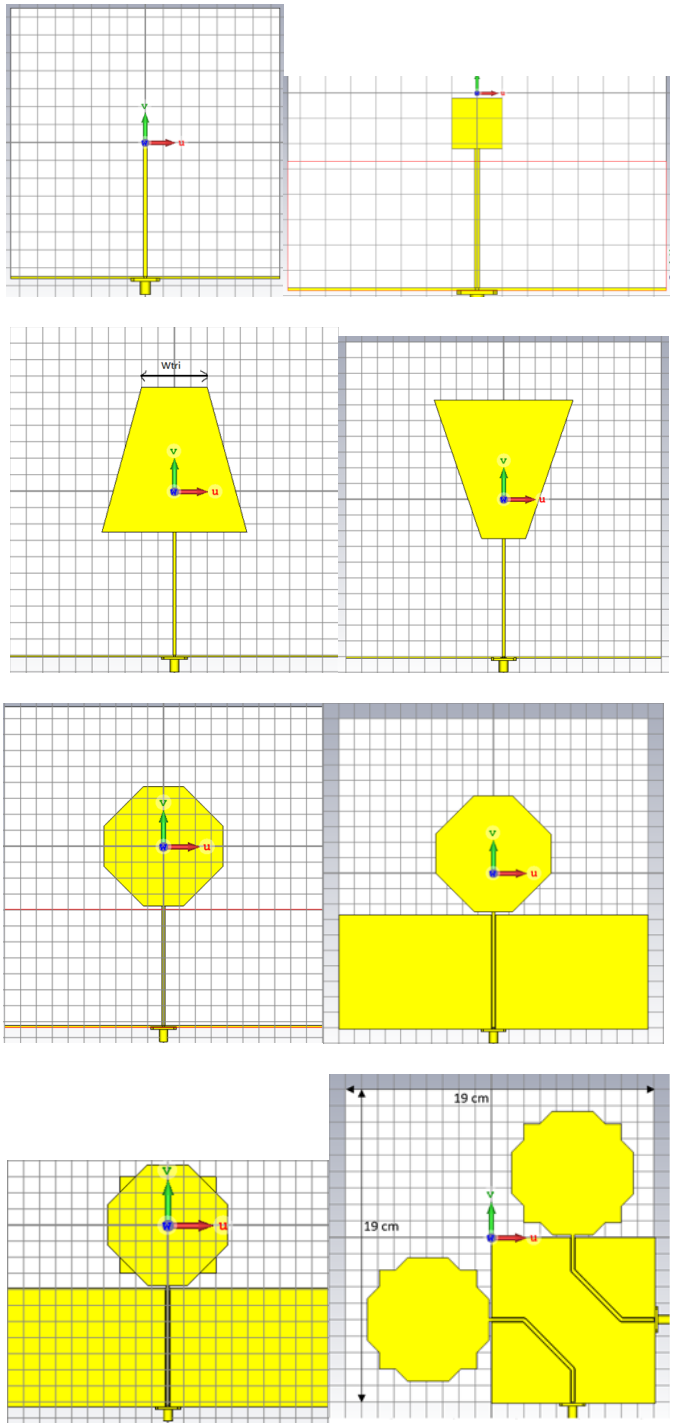


*Figure 5 - Different configurations simulated*

### B. *Monopole with Foam Absorber*

The printed monopole with CPW-feeding and dual linear polarization configuration developed up to this point achieves the required bandwidth between 700 MHz and 3.5 GHz, but since it is a monopole, it has almost omnidirectional radiation pattern and radiates to both the front and back planes.

The monopole is meant to be used integrated in a professional safety vest that is coated with a metallic shielding film. One solution to overcome the negative effects of this shield on the monopole performance is to insert a thick layer of lossy material between the monopole and the shield. Naturally,

the monopole's efficiency decreases but, that is not critical for the envisaged application. In fact, if the efficiency is know it can be taken into account in the estimation of the incident electromagnetic field.

For the lossy material, two absorber foams have been considered, one of them was not known but was available in the laboratory of IT/IST (CF) and the other one was fabricated by Laird. The absorber foam from Laird available in the laboratory, is the Eccosorb AN-75. It is made from polyurethane foam that is treated with special filler and assembled in a laminate construction to generate a controlled conductivity gradient.

*Figure 6 – Multi-layer gradient Eccosorb AN-75*

*Figure 7 – Setup for the experimental macroscopic characterization of Eccosorb AN-75*

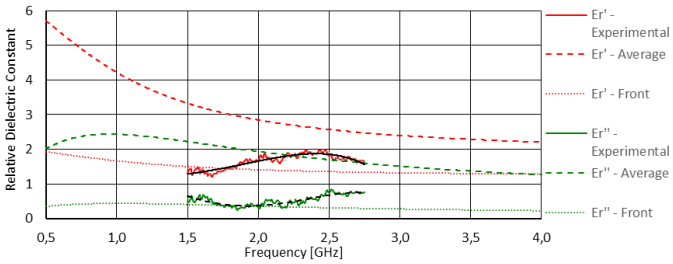


*Figure 8 – Comparison of theoretical and experimental Eccosorb AN-75 characteristics*

From figure 8, it is possible to identify clear differences between the experimental values of $\varepsilon_r$ and the average of the theoretical values. It is noticeable that the experimental εr' and $\varepsilon_r$'', are relatively similar in terms of values to the lines that corresponds to the front layer of the Eccosorb AN-75, $\varepsilon_r$'- Front and $\varepsilon_r$''- Front. The measured data have a reasonable similarity but not in terms of behaviour because a different type of absorber variation is observed.

The CF foam has 30 mm of thickness, and has been tested in the same way of Eccosorb AN-75, in order to characterize its dielectric constant as shown in figure 9.

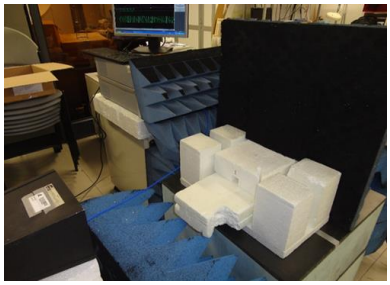

*Figure 9 – Setup for the experimental macroscopic characterization of CF absorber*

In figure 10 is presented a comparison between the experimental values of εr measured for Eccosorb AN-75 and the experimental values of $\varepsilon_r$ measured for CF foam. It turns out that the CF foam introduces more losses due to a higher value of $\varepsilon_r$''.

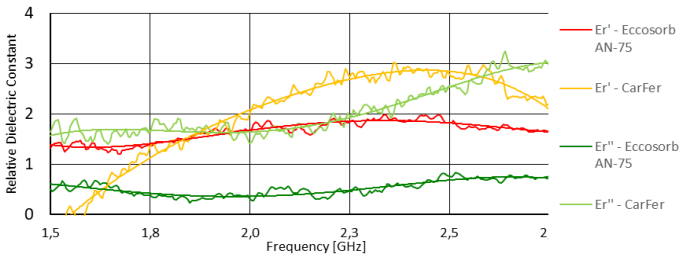


*Figure 10 – Comparison between experimental characteristics of Eccosorb AN-75 and CF absorbers*

Since the CF foam is not in the CST material library, in order to continue simulations to optimize the antenna with the foam thickness, it was necessary to choose witch layer of the Eccosorb AN-75 would be used for the simulations in CST. In terms of the CST models for the Eccosorb AN-75, the layer that is more similar to the CF absorber is the middle layer.

Using the dispersive model from middle layer of Eccosorb AN-75, some simulations were made with the last optimized monopole varying the foam thickness. The printed monopole with CPW feed and dual linear polarization is now backed with absorber foam and a shield cooper plate with 1 mm thickness behind. Maintaining all the parameters of the antenna, the foam thickness is simulated between 5 mm and 30 mm in 5 mm intervals.

Compared with the foam-free model, represented in dark blue, for the case with a thickness of 5 mm, the minimum frequency for which $S_{11}$ <-10 dB increases due to proximity coupling between the antenna and the 1 mm thick copper shield behind. Increasing the thickness of the foam, increases the distance between the shield and the antenna, therefore this minimum frequency decreases, creating a peak around 700 MHz. Since the foam used on the simulations, Eccosorb AN-75 middle layer, introduces fewer losses than the CF foam, better results are expected for the prototype tests.

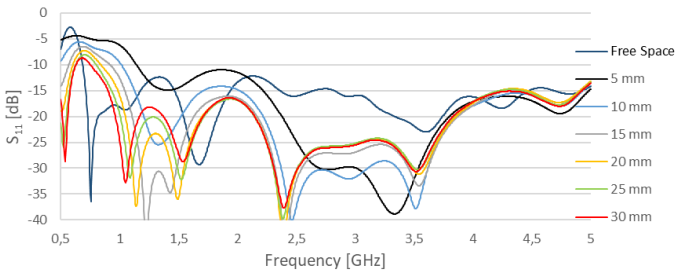


*Figure 11 – Input reflection coefficient for different foam thickness*

### C. Optimized Antenna

The optimized antenna has the following characteristics: The dielectric substrate dimensions are $L_{sub}$ = $W_{sub}$ = 190 mm, the octagonal patch dimensions are $W_{patch}$ = $L_{patch}$ = 75 mm and for the octagonal sides W = 25 mm, L = 35.35 mm and a = 10 mm. The symmetric microstrip lines dimensions are $L_{f1}$ = $L_{f3}$ = 20 mm, $L_{f2}$ = 42.5 mm and $W_f$ = 2 mm, the ground plane dimensions are $W_{gnd}$ = 100 mm, $L_{gnd}$ = 100 mm, the gap between the patch and the ground plane is g = 1.5 mm, and k = 0.4 mm is the gap between the ground plane and the microstrip.

Figure 3.43 shows that for a thickness of the absorber foam of 25 mm, the reflection factor is below -10 dB for all the bandwidth except between 625 MHz and 800 MHz. Therefore, the chosen thickness for the absorber foam was 25 mm, simulating with Eccosorb AN-75 middle layer, since better results are expected with the CF foam.

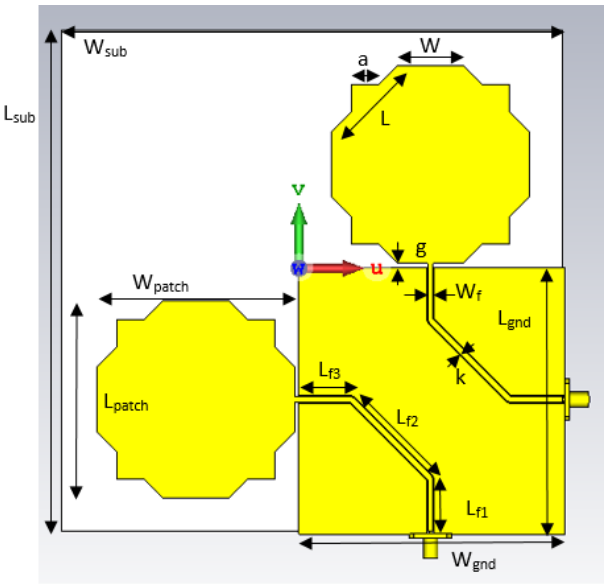


*Figure 12 – Octagonal monopole with CPW feed dual linear polarization backed by absorber foam and shield*

According to the presented results, figure 13, the antenna verifies the criteria of $S_{11}$<-10 dB from 800 MHz to the upper limit of the simulated frequency band, having one peak of -8 dB within the band of interest around 750 MHz. In addition, the average $S_{11}$ of the desired bandwidth of operation is -20 dB, which gives enough margin to guaranty any discrepancies between the simulated and experimental results.

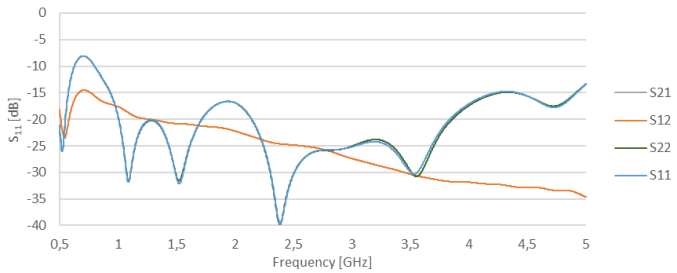


*Figure 13 - S parameters of the optimized dual linear polarization monopole configuration*

Figure 14 shows an average gain of -2.2 dB from 500 MHz to 5 GHz. The negative average gain is expected since the presence of the absorber foam introduces losses. As expected the gain decreases as the frequency increases.

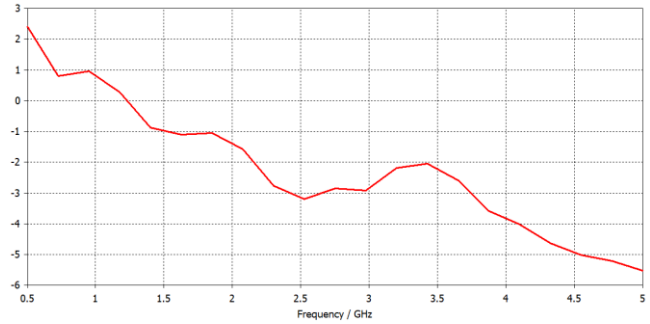


*Figure 14 - Simulated realized gain of the optimized antenna*

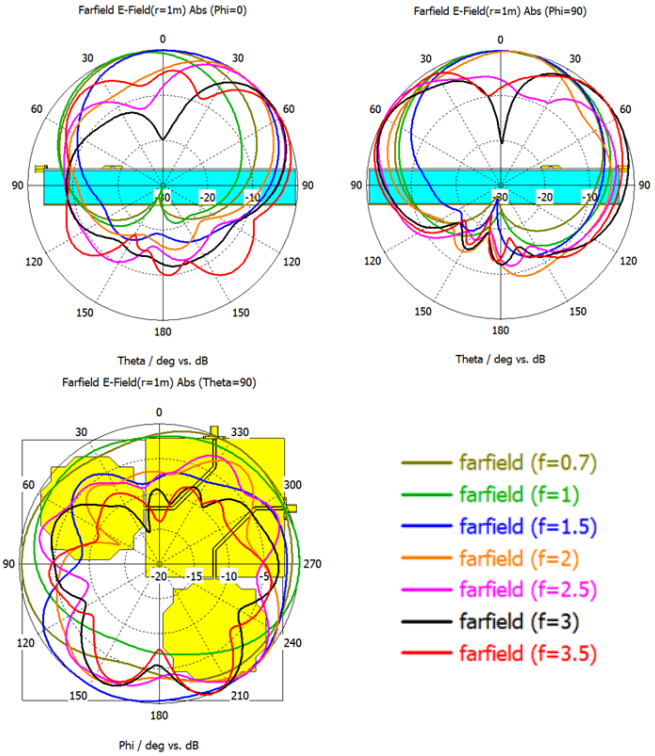


*Figure 15 - Radiation patterns for different frequencies*

Figure 15 represents the radiation patterns for different frequencies between 700 MHz and 3500 MHz. In this case, the power supply is through port 1, due to symmetries the results for port 2 are identical. It is possible to observe in the phi=0°

and phi=90° cuts for the two ports, a strong attenuation in the radiation pattern caused by the absorber foam.

## IV. Antenna Fabrication and Test

### A. Photolithography Fabrication Process

The fabrication process used to manufacture the printed monopole in FR4 was the photolithography technique. It started by producing the masks of the circuit, which is a 2D section of the circuit where the copper (metal part) is represented in black. The masks are then used to print a transparent film of the simulated circuit at a chosen scale. To produce the masks, the author used a script to import a DXF file from CST to further mark the metal parts and then export to PDF, with the defined scale size, for them to be copied into the transparent film.

After the mask is printed and properly aligned, the manufacturing process starts by cutting the dielectric substrate into a square shape and cleaning its surface of any grease or impurities. To apply the pre-treatment, the PCB board is scrubbed with a brush, detergent and water in order to be completely clean.

Once the PCB board is completely clean and dry, the second step was to cover its entire surface with a photoresist solution. This must be done in a room with special light and in a clean, dust-free atmosphere. After applying the photoresist spray, the PCB board was left to dry in the dark for 24 hours. To speed up the process, the author used a thermostatically controlled oven.

The step 3 is very important, as this is where all preparations are made before the unwanted copper areas are exposed to the UV-light. To do that, a positive original transparent film material opaque to light, representing the circuit drawing, was prepared and inserted on top of the PCB board.

Further, in step 4, the circuit is exposed to the UV-light. The time of exposure depends on both the thickness of the coating and on the intensity of the light source.

After that, the next steps 5 and 6, were to remove the film mask and to submit the circuit board to caustic soda and water in dark conditions for the detailed pattern of copper start to appear.

Finally, in the last steps, 7 and 8, is the cleaning process, were the board was immersed in the etchant composed by a mixture of hydrochloric, hydrogenperoxide and water to etch the copper plates and then the softened resist was washed away using an alkaline solution (acetone or another solvent available). At the end, a Soldering Varnish SK 10 was applied to protect the circuit form oxidation and to help the soldering process.

The first prototype produced was the single octagonal patch monopole with cooplanar ground plane configuration. Followed by the second prototype, the dual linear polarization configuration of the previous one shown in figures 17 and 18 respectively.

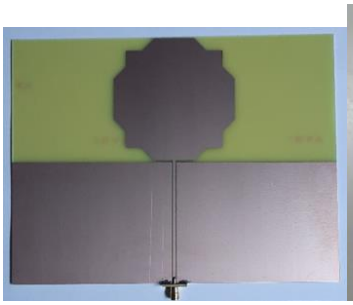

*Figure 16 - First prototype*

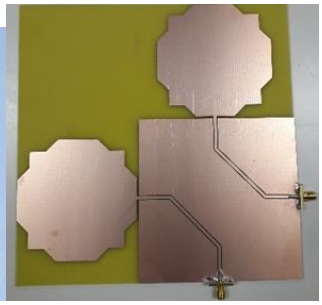

*Figure 17 - Second prototype*

### B. Experimental Results

Figure 20 contains the measured and the simulated reflection coefficient results of the first prototype, the printed octagonal patch monopole with cooplanar ground plane.

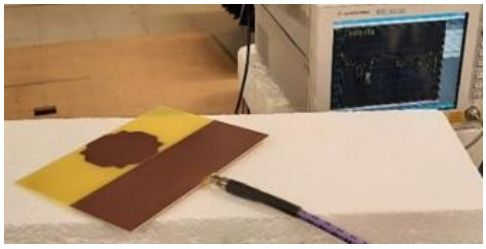

*Figure 18 - S-parameters measurement setup for prototype 1*

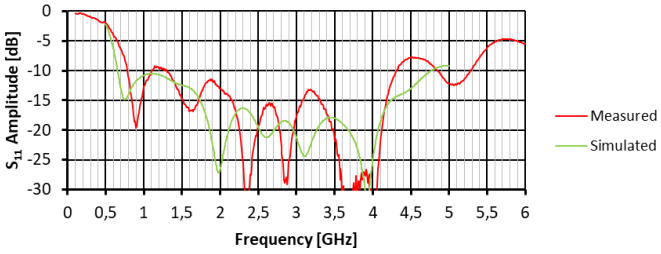


*Figure 19 - Simulated vs measured S11 results of the single octagonal patch monopole*

The simulated and measured results have good agreement and fulfill the requirement of S11 < -10 dB for almost the entire working bandwidth. It is observed in the measured results that the minimum frequency for the condition S11 < -10 dB is higher and there is also a peak slightly above -10 dB around 1.2 MHz.

Regarding the second prototype, three different configurations were tested. The first configuration is the simplest, the antenna is tested without the reflector and the absorber foam in order to validate the simulated results. In the second configuration, the antenna is tested at a distance of 2.5 cm from a reflecting plane without absorber in order to verify its interference. Finally, in the third configuration, the antenna is measured with the selected absorber foam and the reflecting plane.

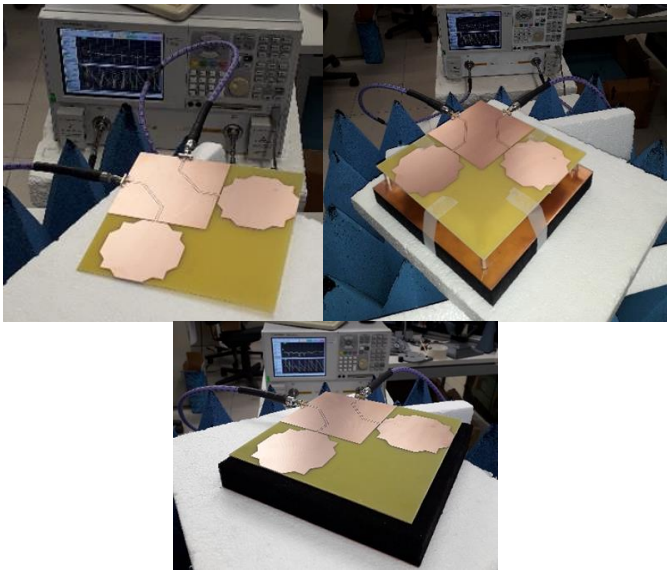

*Figure 20 - S-parameters measurement setup for prototype 2*

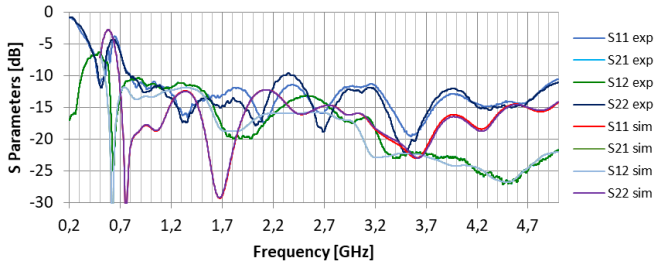


*Figure 21 - Simulated vs measured S-parameters results of configuration 1*

Comparison of simulation and experimental S-parameters results for configuration 1 are shown in figure 22. The measured reflection coefficient $S_{11}$ is below -10 dB from 800 MHz to the end of the working bandwidth while the simulated reflection coefficient in the CST presents lower values in the whole band, as expected.

The difference between the simulated and the experimental results can be caused by the simulator itself (accuracy and mesh used), and by the test environment. In addition, there are always factors that happen during the manufacturing process that can cause these little discrepancies such as the way the antenna was cut, the soldering and connection of the cable that introduce losses and even the materials used, specially FR4 which is not a high quality substrate.

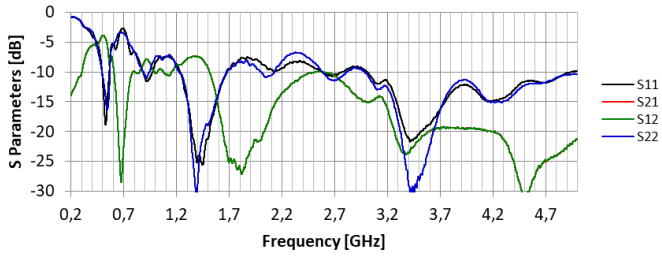


*Figure 22 - Measured S-parameters results of configuration 2*

Figure 23 shows the very negative impact of the reflecting (and shielding) plane in the antenna performance. This negative interference justifies the use of the absorber foam to mitigate it.

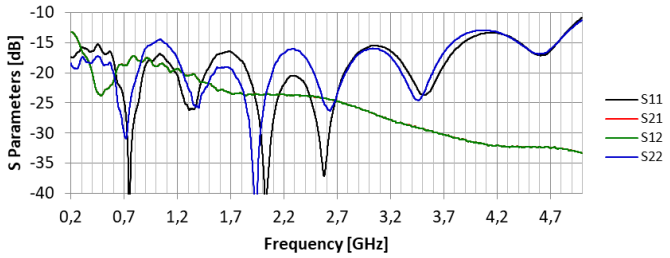


*Figure 23 - Measured S-parameters results of configuration 3*

The absorber foam causes the reflection coefficient to drop below -15 dB across the entire measured bandwidth improving the antenna performance (figure 24). It is therefore confirmed experimentally the expected effect of the absorber foam.

## V. System of Antennas

After the design, optimization and measurement of the printed monopole antenna with absorber foam developed in the previous chapters, a new configuration with spatial diversity is considered. The main objective of this system of antennas is to measure the incident radiation on its user and at the same time protect him from that same radiation. In order to obtain the results of incident radiation around the user, the antennas were placed on the chest, back, shoulders and head, achieving spatial diversity.

The antenna system, shown in figure 26, is composed of five identical printed monopole antennas developed in the previous chapters. To simulate the user's body, the author used a hollow copper block covered with Eccosorb AN-75 (middle layer) of varying thickness between 1 mm and 0,5 mm. All the dimensions of the antenna system are shown in figure 26, where different views of the antennas integrated in the user model are also presented.

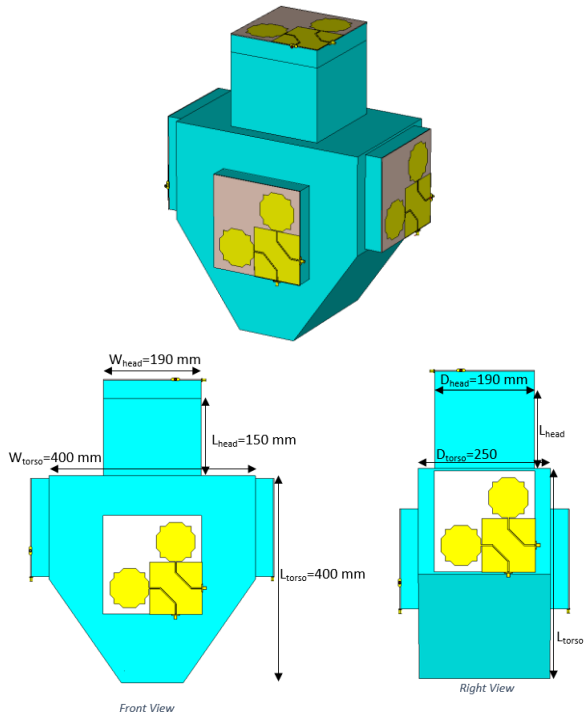


*Figure 24 - System of antennas*

A simple model of the upper part of the user body has been chosen. The head is represented by a parallelepiped with a width and depth of 190 mm but with a height of 150 mm and the chest is represented by a cutted parallelepiped with 400 mm in height and width and 250 mm of depth.

The reflection coefficients for each port were simulated from 700 MHz to 3,5 GHz to verify the impedance matching.

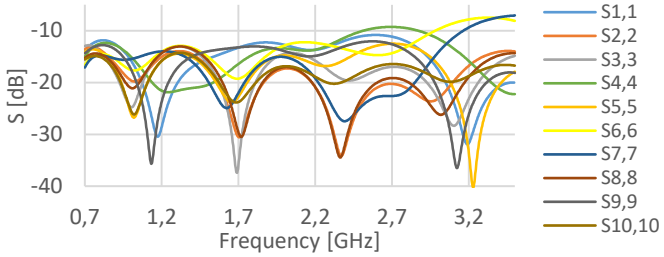


*Figure 25 - System of antennas – S-parameters*

Figure 27 shows the simulated magnitude of the S parameters in dB. According to the presented results, the system verifies the criteria of S < -10 dB from 700 to 3500 MHz for all monopoles except for monopoles 4, 6 and 7. In relation to monopole fed by port 4 there is a maximum of –9,2 dB in the reflection coefficient between 2,51 GHz and 2,87 GHz. In relation to monopoles fed by the ports 6 and 7, the reflection coefficient is slightly above -10 dB from 2,98 GHz and 3,164 GHz, respectively.

Once well matched, the system is no longer fed by the ports but rather excited by a plane wave of 1 V/m from various directions and polarizations. The system was simulated for a phi and theta variation with a range of [0º, 360º[ with 45° intervals.

Using voltage monitors at the SMA connector of each monopole it is expected to observe a higher voltage at the monopoles that are printed on a plane perpendicular to the direction of the incident wave and aligned with the polarization of the incident wave.

A 50 Ω load has been inserted between the inner and outer conductors of the SMA connectors. Therefore, the voltage monitors provide the voltage created on these matched 50 Ω resistance loads.

### *A. Theta Scan (Phi=0)*

Figure 28 contains the antenna system powered by a plane wave with vertical polarization. For the case of the theta sweep from 0 to 315 degrees, only the first three results theta = 0, 45 and 90 are represented for the three types of polarizations since due to (almost) symmetry they provide enough information regarding the voltage at the monopole terminals with the polarization and incident wave direction.

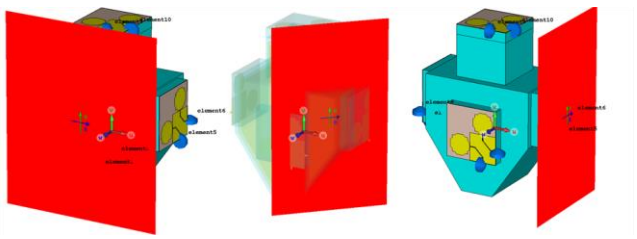

*Figure 26 - System of antennas for theta scan (0°, 45°, 90°) and phi = 0°*

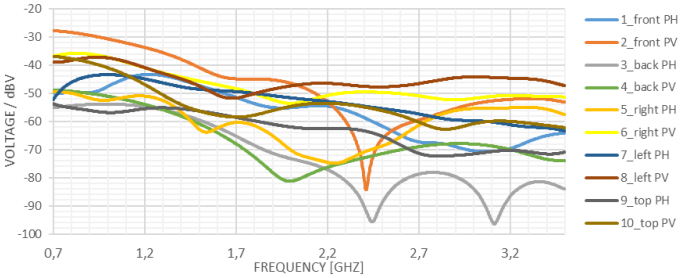


*Figure 27 – Voltage induced at each port for Θ=0° and vertical polarization*

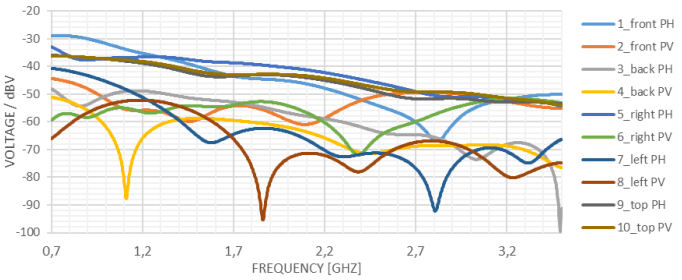


*Figure 28 - Voltage induced at each port for Θ=45° and horizontal polarization*

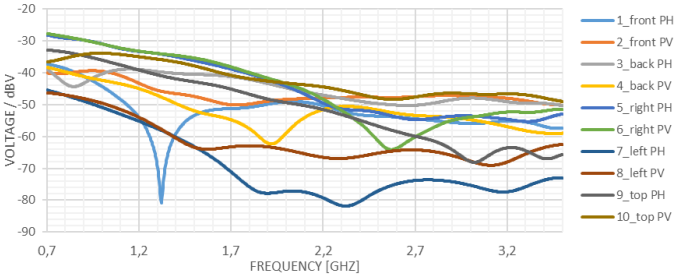


*Figure 29- Voltage induced at each port for Θ=90° and 45° linear polarization*

From the results presented obtained it can be concluded that the monopoles that have higher voltages at their terminals are the ones that are directly in front of the incident wave and that have the configuration of polarization of the incident wave. For example, when the incident wave has a vertical polarization, and Theta=0, the monopoles that present a higher voltage are the front, left, right and top with the vertical polarization configuration. On the other hand, if Theta=45 the monopoles that present higher voltages at their terminals are the front, right and top with the vertical polarization configuration as well. The same behaviour of the system is observed for the other values of Theta and for the case of the incident wave having horizontal polarization.

For the case where the incident wave has linear polarization at 45 degrees, it is observed that the monopoles that present higher voltages at their terminals are the ones that are directly in front of the incident wave. For example, when the incident wave has linear polarization at 45 degrees, and Theta=90°, the monopoles that present higher voltages are the right, back, front and top, regardless of their polarization settings.

In all presented voltage results, there is a decrease as frequency increases caused by the increase of the absorber foam losses. Similar results are observed for phi sweep.

### B. *Incident Electric Field Amplitude Estimation*

The amplitude of the electric field of an electromagnetic wave incident on the antenna system can be estimated using the following procedure:

Read the unloaded voltage of all the monopoles and choose the highest value.

If the frequency of the incident electromagnetic wave is known then the amplitude of its electric field can be estimated from equation

$$E_{est}(f) = \frac{V_0(f)}{\sqrt{G(f)}} \frac{f}{6.164x10^7} \quad (5)$$

using the corresponding gain value obtained in chapter 4.

If the frequency of the incident electromagnetic wave is not known a table of values of the amplitude of its electric field can be estimated, as a function of the frequency (in the range 0.7-3.5 GHz), from equation (5) using the gain values obtained in chapter 4.

It has been assumed that there is a filtering mechanism that allows selection of the received signals in a chosen narrow frequency band. One of the tasks that needs to be carried out to make this procedure more effective is the estimation of its accuracy.

## VI. Conclusions

This thesis describes the study, design, optimization and fabrication of two wideband printed monopole antennas to cover a frequency band starting from 700 MHz to 3,5 GHz, specially challenging due to size constraints. Several of these monopoles will be combined to form an antenna system capable of estimating the unknown amplitude of the electric field received by the user in a professional unknown work environment. The main challenges of the problem under analysis come from the wideband (5:1), the small size and the unavoidable proximity of the antennas from the conducting protective shield.

A historical and scientific review is made about printed antennas, more specifically microstrip patch antennas and printed monopoles. The advantages and disadvantages of their use are discussed, as well as a review of wearable antennas. A detailed parametric study was performed, with all relevant parameter studied such as: monopole width, ground plane dimensions and geometry, dielectric substrate dimensions and patch geometry. Both free space and foam loaded environments have been considered. Moreover, orthogonal dual-linear polarization configuration have been developed.

After the antennas were optimized, meeting the required working bandwidth, a system was developed consisting of five of these printed antennas with absorber foam. A basic model for the user's body was used, simulated with a hollow copper block. The system was powered by a plane wave with an incident angle sweep in theta and phi for vertical, horizontal and linear polarizations at 45 degrees

After being developed, this antenna system can be used to measure the amplitude of the incident electric field on the system user from the voltage obtained at the terminals of each monopole. The voltages decreases with an increase in frequency due to losses and higher voltages are verified for the monopoles where the wave falls in the direction of maximum radiation.

Due to the terrible Covid-19 virus pandemic, there were severe limitations on the experimental work. However, it was possible to fabricate two antenna prototypes and measure their S-parameters. A general agreement between numerical simulation and experimental results was obtained. Such concordance has validated the design procedure and provided proof of the proposed antenna concepts.

There are many aspects that could have been addressed in this work, and there are also many issues that could be investigated to render the work more complete. A non-exhaustive list of future work topics is suggested below.

- Measurement of the radiation pattern (and associated parameters) of the fabricated prototypes in a anechoic chamber.
- Analysis of the polarization properties of the monopoles developed.
- Estimate the accuracy of the proposed estimation procedure of the amplitude of the incident electric field provided by the developed antenna system.
- Investigate the effects of increasing the number of dual-linear polarization monopoles and the best location for them.
- Investigate the effects of the bending of the monopoles caused by the integration into the vestment.
- Investigate the effects of the textiles of the garment that cover the antennas.

## VII. Acknowledgments

The author would like to express his sincere gratitude to Professor Custódio Peixeiro for the continuous support during this thesis, for his patience, dedication, knowledge and guidance. To Mr. Carlos Brito and Professor Carlos Fernandes, for their knowledge, experience and participation in the fabrication and test of the prototypes. A special thanks to the author´s parents, brother and friends, for their unconditional encouragement and support during this journey. To Instituto Superior Técnico (IST), a school filled with science and knowledge, where the author completed his studies. Finally, a very special thanks to Instituto de Telecomunicações (IT), the institution that sponsored and hosted this thesis.

## VIII. References

[1] [online accessed] https://www.centi.pt/projetos/texteis-avancados/ipvest-centi-nanotecnologia

[2] C. A. Balanis, “Antenna Theory Analysis and Design.”, 3rd Ed., John Wiley Sons, Inc., Hoboken, New Jersey, 2005.

[3] J. Q. Howell, "Microstrip Antennas," IEEE Transactions on Antennas and Propagation, Vol. 23, pp. 90-93, 1974.

[4] K. Mandal, “A Review on Printed Monopole Antenna for UWB Applications”, International Journal of Advanced Research in Computer and Communication Engineering, Vol. 4, December 2015.

[5] C. Oliveira, “Characterisation of on-body Communications”, PhD Degree Thesis, Instituto Superior Técnico 2013.

[6] [46] C. Mendes, “A Wearable Dual-Mode Printed Antenna for Body-Centric Applications”, PhD Degree Thesis, Instituto Superior Técnico, 2017.